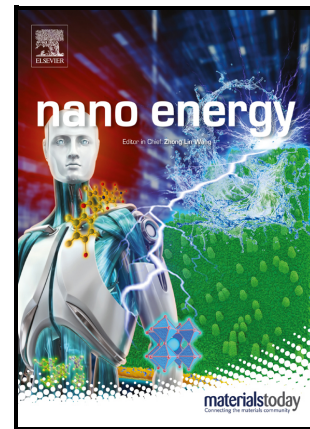


Wearable Five-finger Keyboardless Input System
Based on Silk Fibroin Electronic Skin

Jiarong Liu, Jianfeng Chen, Fukang Dai, Jizhong Zhao, Shengyou Li, Yating Shi, Wanjing Li, Longyu Geng, Meidan Ye, Xiaping Chen, Yufei Liu, Wenxi Guo



PII: S2211-2855(22)00841-2

DOI: <https://doi.org/10.1016/j.nanoen.2022.107764>

Reference: NANOEN107764

To appear in: *Nano Energy*

Received date: 13 August 2022

Revised date: 30 August 2022

Accepted date: 30 August 2022

Please cite this article as: Jiarong Liu, Jianfeng Chen, Fukang Dai, Jizhong Zhao, Shengyou Li, Yating Shi, Wanjing Li, Longyu Geng, Meidan Ye, Xiaping Chen, Yufei Liu and Wenxi Guo, Wearable Five-finger Keyboardless Input System Based on Silk Fibroin Electronic Skin, *Nano Energy*, (2022) doi:<https://doi.org/10.1016/j.nanoen.2022.107764>

This is a PDF file of an article that has undergone enhancements after acceptance, such as the addition of a cover page and metadata, and formatting for readability, but it is not yet the definitive version of record. This version will undergo additional copyediting, typesetting and review before it is published in its final form, but we are providing this version to give early visibility of the article. Please note that, during the production process, errors may be discovered which could affect the content, and all legal disclaimers that apply to the journal pertain.

© 2022 Published by Elsevier.

Wearable Five-finger Keyboardless Input System Based on Silk Fibroin Electronic Skin

Jiarong Liu, Jianfeng Chen, Fukang Dai, Jizhong Zhao, Shengyou Li, Yating Shi, Wanjing Li, Longyu Geng, Meidan Ye, Xiaping Chen*, Yufei Liu* and Wenxi Guo*

J.R. Liu, J.F. Chen, J.Z. Zhao, S.Y. Li, Y.T. Shi, W.J. Li, L.Y. Geng, Prof. M.D. Ye, Prof. X.P. Chen, Prof. W.X. Guo

Research Institute for Biomimetics and Soft Matter, College of Physical Science and Technology, Jiujiang Research Institute, Fujian Provincial Key Laboratory for Soft Functional Materials Research, Xiamen University, Xiamen, 361005, China

E-mail: wxguo@xmu.edu.cn (W.G.); chenxp@xmu.edu.cn (X.C.)

F.K. Dai, Prof. Y.F. Liu

Key Laboratory of Optoelectronic Technology & Systems (Chongqing University), Ministry of Education, Chongqing 400044, China

E-mail: yufei.liu@cqu.edu.cn (Y.L.)

Keywords: silk fibroin, electronic skin, wearable device, input method, human-computer interaction

Abstract

To get rid of the limitations of traditional keyboards, we report a new generation wearable keyboardless input system (WKIS). Based on the coupling of triboelectrification and electrostatic induction, the single-electrode mode triboelectric nanogenerator (TENG) worn on the five fingers can convert finger tapping into electrical signals. Meanwhile, by developing a number pair coding table in vowel mode, we integrated the 26 English letters and necessary instructions into WKIS with five-finger tapping. The main body of the device is an ultra-thin silk fibroin film (SF), which is biocompatible, water-permeable, breathable and skin conformal, enabling it suitable for long-term wear as a ring on the finger. Data coding and transmission process are completed through a printed circuit board (PCB) and Wi-Fi module to realize keyboard communication. Feature engineering and machine learning are employed to identify WKIS registered users with an accuracy of 92%. In addition, the WKIS provides an effective solution in smart home control, which has potential applications in future human-computer interaction, Internet of Things and VR scenarios.

1. Introduction

With the development of the Internet of things, many wearable devices with human-computer interaction have poured into people's vision. Input system is an important link hub of human-computer interaction of wearable devices[1–3], which can control various equipment such as robots[4,5], household devices[6–8], musical instruments[9–11] etc., through a flexible coding system. Input devices such as wearable keyboards will provide more possibilities for improving the controllability of human-computer interaction and expanding wearable application scenarios. In 1868, Christopher Latham Sholes designed the first commercial typing keyboard, decades before the emergence of computers[12]. With the gradual popularity of visual terminal computers over the last century, companies such as IBM introduced the current standard keyboard with neater keys[13] (Figure. 1a). The emergence of the keyboard promotes the popularization of the computer, realizes smooth human-computer interaction, and becomes an essential input device. The development of the modern keyboard gradually takes into account the convenience of equipment, based on this, the third generation of keyboard-laser projection keyboards emerged[14]. The keyboard's laser can project a full-size keyboard on a flat desktop, but requires an optical environment and a projection surface, making it difficult to popularize. With the application of nanotechnology in wearable devices, flexible matrix keyboards based on flexible pressure sensors have become the fourth generation of keyboards[15–17]. Based on flexible materials, an array of mechanical sensors is constructed to sense finger tapping. Yang Kyu Choi's group proposed a fabric-based flexible triboelectric nanogenerator keyboard[18]. Each unit in the keyboard generates an electrical signal according to the external touch, and after proper data filtering, the high-precision text input can be realized. Dong's team proposed a non-contact receiving keyboard using a new resonant triboelectric nanogenerator[19]. Each key on the keyboard combines TENG, coil, and external capacitance to generate oscillating signals, which are tuned to different oscillating frequencies to identify the key pressed. Wang's group has developed a pressure-enhanced keyboard with a security system[20]. Tactile sensors can convert typing into electrical signals and identify users through their unique typing behaviour.

The matrix keyboards are limited by the traditional keyboard design concept, inconvenient to carry, limited functions. Creating a simpler, versatile wearable keyboard requires at least three efforts. First of all, in terms of materials, the electrode is required to be light-weight, low-cost, good skin-friendly, and skin conformal, suitable for long-term skin adhesion. Second, it is necessary to develop a completely new input method to replace the traditional input habit, get

rid of the use of matrix keyboard, and achieve keyboardless input. Finally, with the rapid development of artificial intelligence, wearable input system needs to have better compatibility and scalability, and be suitable for more application fields when combined with machine learning.

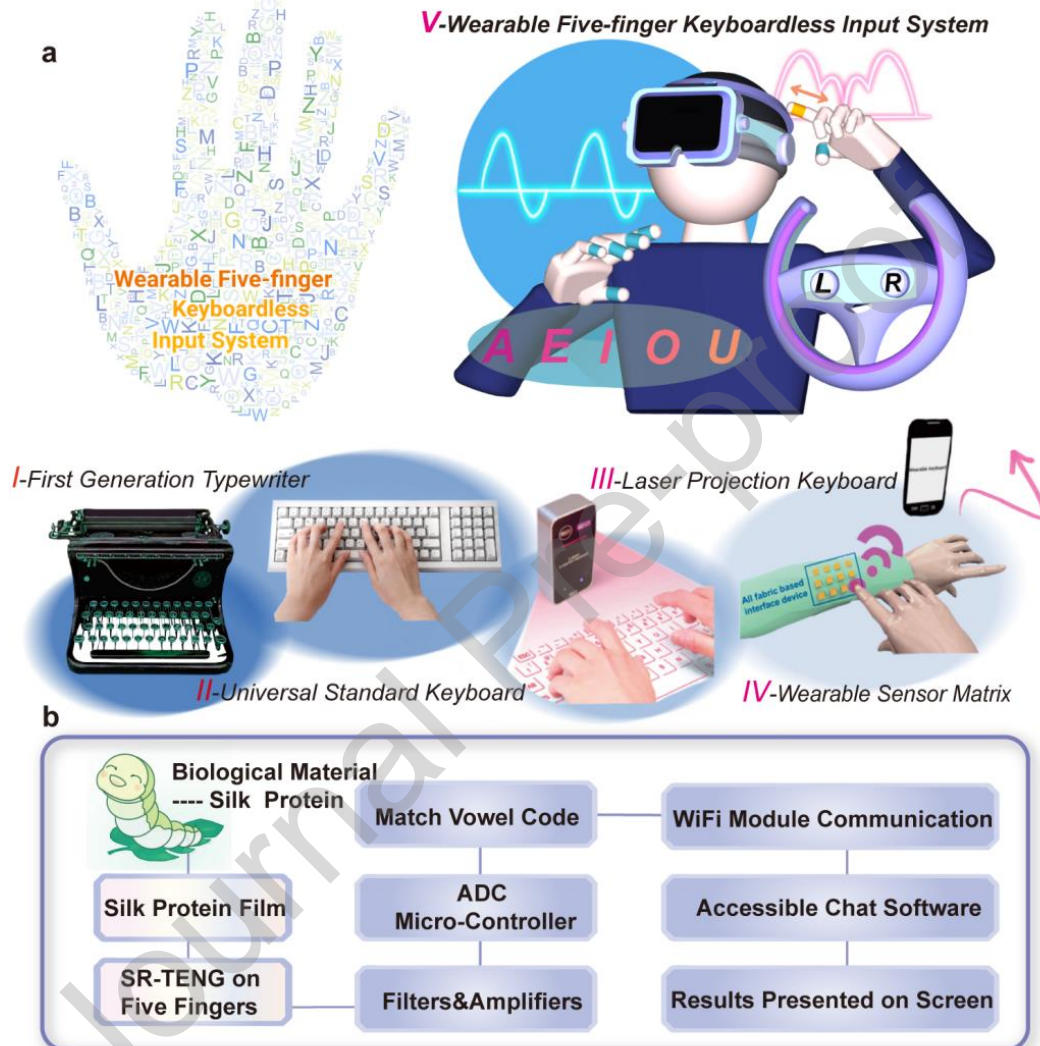


Figure 1. The concept of the whole WKIS. (a) The development of wearable keyboard. (b) The back-end design of the whole WKIS.

Here, we developed a new generation keyboard based on silk fibroin (SF) rings and a five-finger wearable keyboardless input system (WKIS). First of all, a soft and ultra-thin SF film with good biocompatibility, air/water/sweat permeability, and conformability was prepared as a friction electrode for long-term skin contact. Second, in device design, we introduce a single-electrode mode SF ring triboelectric nanogenerator (SR-TENG), which can produce electrical signals in contact with other objects without an external power supply. Finally, on

the basis of the WKIS coding system, we created a number pair coding table of vowel mode, incorporating 26 English letters and some other necessary instructions into the five-finger input device, through data processing, data coding, data wireless transmission and machine learning, realize the communication function of WKIS (Figure. 1b). In addition, we expanded the application of the wearable keyboard to identify WKIS registrants using a support vector machine (SVM) algorithm through the characteristic model of signals generated by different users. The combination of directional and coding function of WKIS provides an efficient solution for smart home control. Our WKIS may become promising to find potential applications in human-computer interface, business, VR scenes and other fields in the future.

2. Results

2.1. Materials and structure design

Biocompatibility and skin comfort are very significant for long-term wearing devices. Here, SF, a natural biomaterial, is attached on the finger and accurately captures the mechanical energy of the finger strike into the corresponding electrical signal. As shown in Figure. 2a, SF is prepared by the process of degumming, dissolving, dialysis, and evaporation solution steps, as previously reported[21–23]. Silver nanowires were uniformly coated on the SF membrane as the electrode, which is protected by being packaged with another SF membrane (Figure. 2b). The silver nanowires have good light transmittance, which can improve the aesthetics of electronic skin in design. To adapt to the fingers, the thickness of the device is only $\sim 38 \mu\text{m}$ with an effective size of $1 * 1\text{cm}^2$ (see Figure. S1). To further improve the skin conformal of the TENG ring, silk is mixed with the enhancer in the ratio of 1:500 and evaporated naturally to form a modified SF film. The modified SF film demonstrated better tensile properties (150% strain, 8 Mpa stress) than pure SF film (Figure. 2d). Previously, it is reported that both the glycerol doping and steam annealing treatment could give rise to the conformation transition from α -helix/random coil to β -sheet, leading to the enrichment of the β -crystallites[24–26]. It can be proved from the small-angle X-ray diffractometer (XRD) pattern (Figure. 2c) that the crystallinity of modified SF film is higher than that of pure one. Besides excellent conformal property, good light transmittance is beneficial to the visual stealth of wearable devices. As shown in Figure. 2e, the optical transmittance of SF film at the wavelength of 300 nm-1000 nm is higher than 90%, wearing on the fingers has more beautiful and concealment. As for biocompatibility, after attaching our sensor on the skin for seven days, no swollen and allergic reactions were observed as shown in Figure. 2g. Sweat

immersion and water permeability tests proved that the device has good water permeability and stability in sweat (Figure. S2&S3).

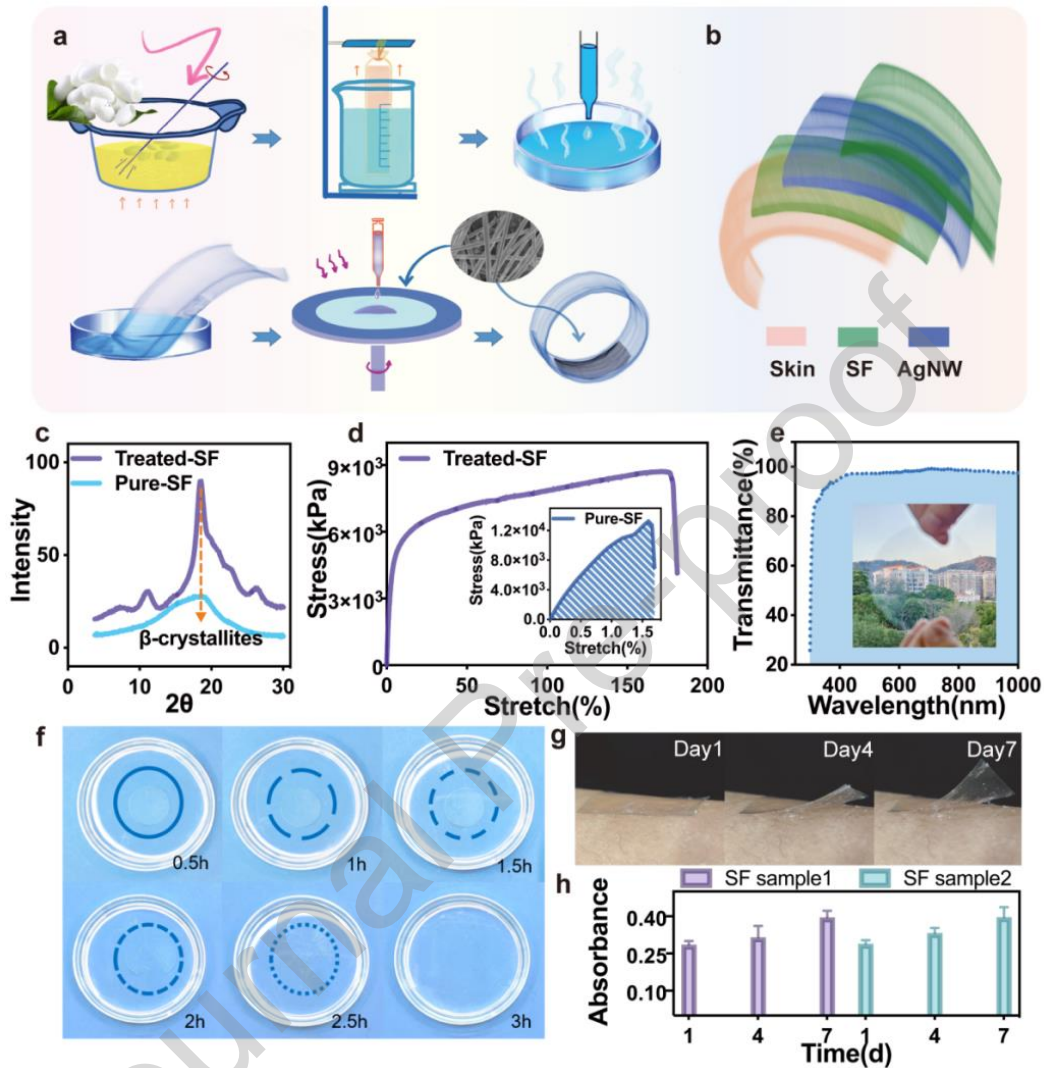


Figure 2. The preparation and properties of electrode materials. (a) Preparation process of silk fibroin film for SR-TENG. **(b)** The structure of SR-TENG. **(c)** XRD of pure and modified silk fibroin films. **(d)** Tensile properties of pure and modified silk fibroin films. **(e)** Light transmittance of modified silk fibroin films. **(f)** Image of the gradual degradation process of modified silk fibroin film within 3 hours. **(g-h)** Biocompatibility of modified silk fibroin films.

To further investigate its cytocompatibility, we used the CCK-8 cell counting method to detect the viability and proliferation ability of mouse preosteoblasts (MC3T3-E1) after one week of culture on SF. After 4 days of incubation, cell number largely grows to high density on the SF samples that cell size decreases. On day 7, cellular density becomes even higher due to the confluent cell monolayer forms with cell clusters (Figure. 2h). The results indicate that MC3T3-E1 cells exhibit good attachment, spreading, and growth on the SF. In addition,

we tested the degradation of the devices, as shown in Figure. 2f, the device completely disappeared after soaking in 5% papain solution for 3 h. This is because papain can destroy the structure (hydrogen bond) of silk fibroin, hydrolyze the peptide bond into amino acid residues and accelerate the degradation of the material[27].

2.2 Characterization of mechanical and electrical properties of SR-TENG

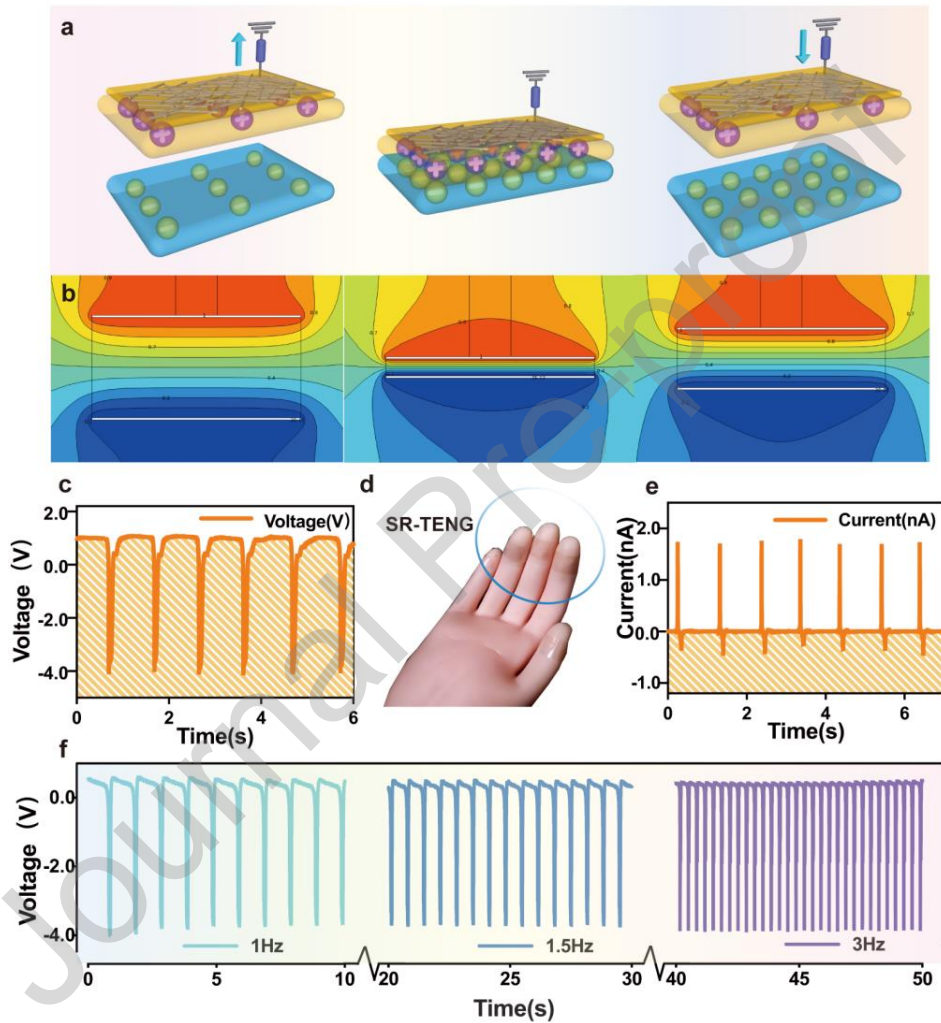


Figure 3. The Characterization of mechanical and electrical properties of SR-TENG. (a-b) The basic working mechanism of SR-TENG explained by space simulation and Comsol simulation. (c-e) The open circuit voltage (V_{OC}) and short circuit current (I_{SC}) of SR-TENG ($1 \times 1 \text{ cm}^2$) on the finger. (f) The open circuit voltage (V_{OC}) of SR-TENG ($1 \times 1 \text{ cm}^2$) at different frequencies.

In order to promote the wearability of the device, the SR-TENG is designed as a single-electrode mode, that is, only one electrode is connected to the triboelectric layer (called the main electrode), and the other electrode is used as a potential reference, which can be placed anywhere, or even directly grounded (called the reference electrode)[28,29]. Figure. 3a and

Figure. 3b illustrate the basic working mechanism of SR-TENG through spatial simulation and finite element electric field simulation respectively. Considering the excellent insulation properties and contact electrification properties of the material, it can be assumed that the charges are uniformly distributed across the surface on a macroscopic scale, and the attenuation can be ignored. When the finger-mounted SR-TENG beats the reference electrode at a constant speed, the two are superimposed face to face, forming a triboelectric couple. When they are close to each other, due to the electronegativity difference of materials, an equal amount of surface positive and negative charges “Q” are generated, forming a potential difference between the two poles, and current flows from SR-TENG to the test terminal (grounding). Next, when the two continue to approach until they contact each other, the accumulation of induced charge reaches a maximum equilibrium state, at which point the current approaches zero and produces a reverse peak in the external circuit; As the two contacts gradually separate, the induced charge of the interface layer of SR-TENG decreases, and the potential difference and reverse current are generated again. The electrical measurement results as shown in Figure. 3c&Figure. 3e display that an open circuit voltage (V_{OC}) of 4 V and a short circuit current (I_{SC}) of 1.8 nA are achieved when a finger wears a SR-TENG with $1 * 1\text{cm}^2$ and strikes the PTFE at a frequency of 1 Hz (Figure. 3d). To stably integrate SR-TENG into the system, the outputs are required to be stable, durable and reproducible. V_{OC} variations were measured when SR-TENG was operated at different frequencies over 100 cycles. Although higher operating frequencies (less charge transfer time) will lead to faster charge transfer between electrodes, thus increasing the output voltage. However, it turns out that when the human finger stroke frequency increases from 1 Hz to 3 Hz (following the rhythm of a commercial metronome), the output voltage remains a stable output of 4 V (Figure. 3f), which may be due to the complete polarization of friction charge caused by the small surface area of the contact surface. SR-TENG can maintain stable voltage and current output after 30 days, providing the stability of wearable devices for long periods of operation (Figure. S4).

2.3 Directional function of WKIS

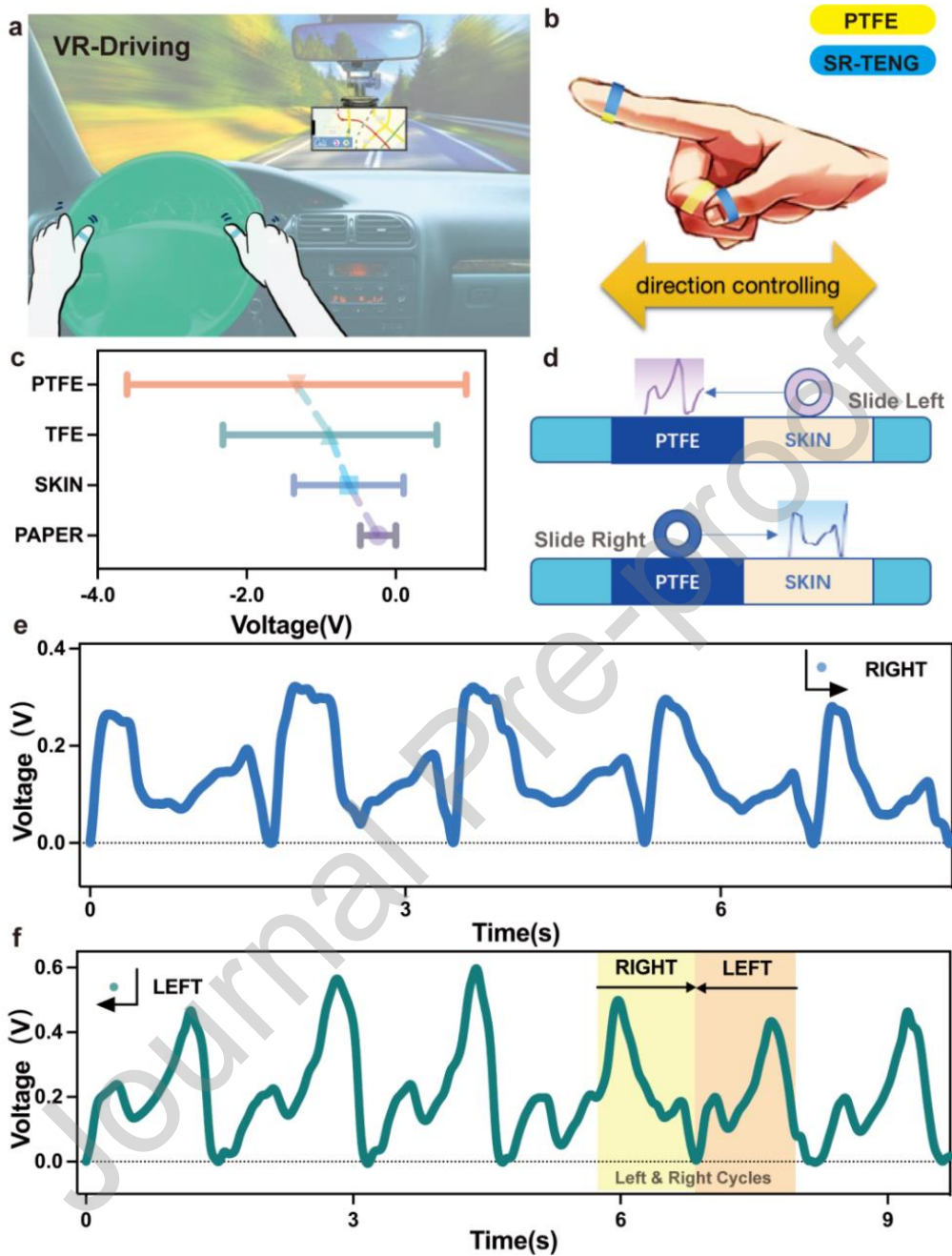


Figure 4. The direction control of flexible WKIS. (a) The direction control function is applied to the concept of VR game driving. (b) SR-TENG realizes direction control function by finger sliding. (c) Voltage variation range of SR-TENG in contact with different materials. (d) Principle demonstration of direction function realization. (e) Voltage change waveform generated by SR-TENG when the direction is to the left. (f) Voltage variation waveform generated by SR-TENG during direction switching.

The difference in electronegativity between TENG electrodes is used to ingeniously realize the directional selection function of WKIS, which can replace the steering wheel in virtual reality (VR) games, as shown in Figure. 4a. Left-right control can be achieved by sliding the SR-TENG worn on the thumb relative to the PTFE ring on the index finger or the skin of the middle finger (Figure. 4b). This is because the electronegativity of human skin and PTFE material is very different, so the voltage generated by SR-TENG contacting with PTFE is significantly greater than that generated by contacting with human skin[30]. As shown in Figure. 4d, when SR-TENG first contacts the skin interface and slides to the PTFE interface from left to right, a left chiral peak voltage with a first small and then large waveform transformation is generated. On the contrary, when SR-TENG first contacts the PTFE interface and slides to the skin interface, the right chiral peak voltage with the first large and then small waveform transformation is generated. Here, the clever use of skin as a contrast electrode can simplify the structure of the wearable system and improve the user experience. Figure. 4e and 4f respectively show voltage curves generated by sliding friction in opposite directions, both of which have good repeatability. Since the signal waveforms generated by sliding in two opposite directions are almost symmetrical, the sensitivity of direction switching depends on the speed of signal generation, that is, the volunteer's speed of the SR-TENG sliding with the skin/PTFE. By changing the sliding direction, an almost symmetrical curve can be obtained (Figure. 4f), indicating that WKIS can realize the function of mouse direction selection. In the future, we can add more direction and angle controls, simplify complex and heavy game-pads and VR controllers, and apply them to virtual reality.

2.4 Coding function of WKIS

In order to achieve the text input function, we have developed a unique wearable input method based on five-finger strokes as shown in Figure. 5. Due to the V_{OC} of the device worn on the hand is dependent on many factors, to avoid mistyping, the input voltage threshold needs to be defined. It is obvious from Figure. 5a and 5b that the V_{OC} increases with the increase of device area and thickness, respectively [31]. In addition, due to differences in the natural strength, height, and speed of human fingers at the keyboard, we collected the average of the maximum voltage of the volunteers' five fingers at 60 times of natural strength. As shown in Figure. 5c, the signal generated by the thumb is significantly stronger than that of other fingers, while that generated by the little finger is the smallest. Therefore, in the back-end design, the output voltage signals of different fingers should be scaled in different proportions so as to be numerically close.

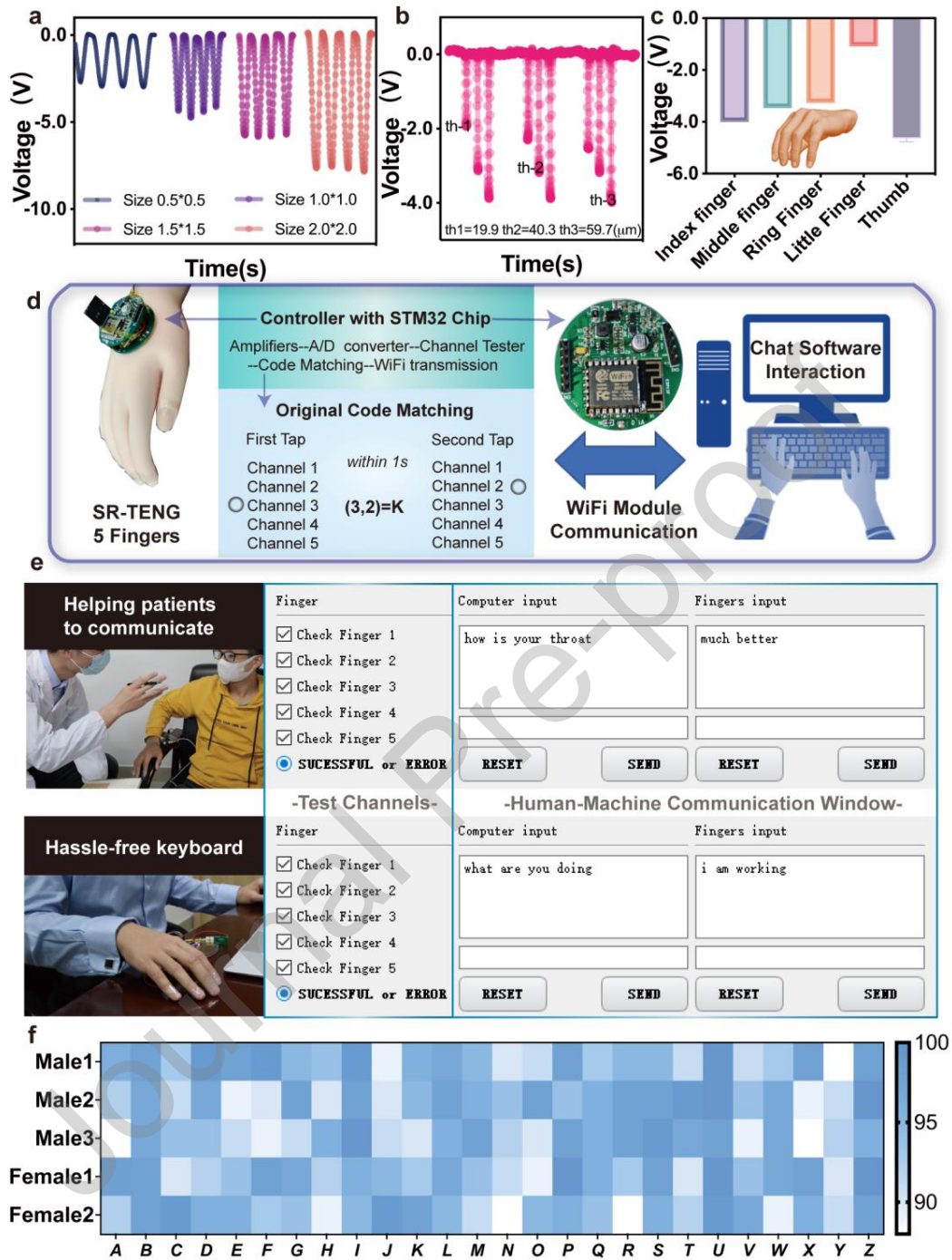


Figure 5. The coding function of flexible WKIS. (a) Relationship between the output voltage of SR-TENG and device area and thickness. **(b-c)** The average value of the maximum voltage of 5 fingers tapping the SR-TENG with natural force for 60 times. **(d)** WKIS system input flowchart.. **(e)** WKIS is used in the workplace and doctor-patient communication scenarios with barrier-free chat windows. **(f)** Correct rate distribution of 26 letters struck by different testers.

Table 1 Number pair coding table in vowel mode

Finger	0 Switch	1 Thumb	2 Index	3 Middle	4 Ring	5 Little
Thumb 1	A-(1,0)	B-(1,1)	C-(1,2)	D-(1,3)	Delete	Send
Index 2	E-(2,0)	F-(2,1)	G-(2,2)	H-(2,3)	Reset	Space
Middle 3	I-(3,0)	J-(3,1)	K-(3,2)	L-(3,3)	M-(3,4)	N-(3,5)
Ring 4	O-(4,0)	P-(4,1)	Q-(4,2)	R-(4,3)	S-(4,4)	T-(4,5)
Little 5	U-(5,0)	V-(5,1)	W-(5,2)	X-(5,3)	Y-5,4	Z-(5,5)

Specifically, the signals generated by 5 fingers tapping are encoded and converted into keyboard letters according to Table 1. The whole coding table takes vowel letters “A/E/I/O/U” as switch letters, corresponding codes are 1, 2, 3, 4, and 5, respectively. When the user clicks his finger for the second time within 1s, the corresponding code is generated to display the matching letter. For example, if tapping the middle finger immediately after tapping the index finger, the letter “H” corresponding to code (2, 3) will display. If there is no double-tap within 1s, the value feedback is 0 and only vowels A/E/I/O/U are displayed. For example, tapping index finger 2 and then pausing, the letter E corresponding to code (2, 0) is displayed. Based on this unique input method, we built an entire operational logic of the wearable system as shown in Figure. 5d, in which SR-TENG can generate the original signal through the finger tapping interface, then input the signal into STM32 for a series of data processing and coding processes, and send the control signal through the Wi-Fi module, the upper computer (Figure. S5) receives the signal for generating feedback, and finally outputs letters in the display panel (see Supplementary Movie 1). As can be seen from Figure. 5e, the WKIS can provide barrier-free communication for deaf people and other patients who cannot speak. In the process of using, the user first activates the upper computer by simple finger tapping to check whether the five fingers are connected smoothly. Then, the user enters the required statement according to the code in the finger input interface. To facilitate use, the functions of space-key, deletion, and recharge are also provided. For example, as shown in Figure. 5f, when a doctor asks a patient who can't speak, the patient could use the WKIS to express his or her thoughts precisely, and the corresponding video demonstration can be found in Supplementary Movie 2. Considering the differences in typing habits and the dexterity of different fingers, we invited 5 volunteers to use our WKIS to type 100 times from A to Z, with an accuracy rate of more than 90%. Of course, increasing typing proficiency can further improve typing accuracy.

2.5 Security defense and private information protection

Keystroke dynamics is a behavioral biometric technology based on human typing attributes[32] Its ballistic properties and non-invasive monitoring characteristics promote its application in multifactor authentication[33,34]. However, most academic and industrial studies only use the characteristics of keystroke delay and keystroke holding time, without considering individual typing force, typing speed and finger size[18]. As an on-skin wearable keyboard, our device can be used for biometrics by capturing more input details than a traditional keyboard. We invited 5 volunteers (3 men and 2 women) and collected their current signals generated by tapping as shown in Figure. 6a&Figure. S6. According to the characteristic parameters, the algorithm preliminarily calculates the *Spearman* correlation coefficient between the five users to evaluate the data correlation between the two users (Figure. S7). The correlation coefficient between the five users and themselves is close to 1, but the correlation with other users is very small. This eliminates miscellaneous information for our machine learning calculation and filtering the eigenvalues such as typing frequency and extreme value of response voltage with obvious population differences (Figure. 6b), which provides the basic direction of model feature selection. We collected 2000 current data generated by 5 subjects, 80% of which were used as training set and 20% as test set, a multi-classification SVM algorithm was used to classify the current data, adjusted the parameters of the SVM algorithm, and improved the accuracy of classification. SVM is more accurate than other common nonlinear-classification models (KNN/NB/CART) in Figure.S8 because it can map linearly non-separable data in the input space to a high-dimensional feature space by kernel functions that make the data linearly separable in the feature space.

In this experiment, the Radial Basis Function(RBF) kernel is used as the kernel function of the algorithm, since the RBF kernel can map samples to a higher-dimensional space[35,36], which is very suitable for processing samples in the case of the nonlinear relationship between class labels and features. When using the RBF kernel, the penalty coefficient C should be considered. To avoid the over-fitting problem caused by too large C value and the increasing possibility of misclassification caused by too small C value, we use k-fold cross-validation to improve the accuracy of the predicted classification and help to find the most appropriate parameter C in the model. We adjusted the value of parameter C to 1.0 1.3 1.5 1.7 2.0 and calculated the prediction accuracy and deviation range of the model, as shown in Figure. 6c, where the highest accuracy of the system predicted classification was close to 90%. The

recognition rates for the five subjects could reach 90%, 100%, 85%, 90% and 95% respectively. The confusion matrix is shown in Figure. 6d. Through the SVM classifier created by the final training, we can recognize who is using the WKIS. When the user data is entered into the machine learning model, we can match whether it is a registered user of the system, and help the WKIS to add a lock-in security defense and private information protection.

2.6 Application of WKIS in smart home

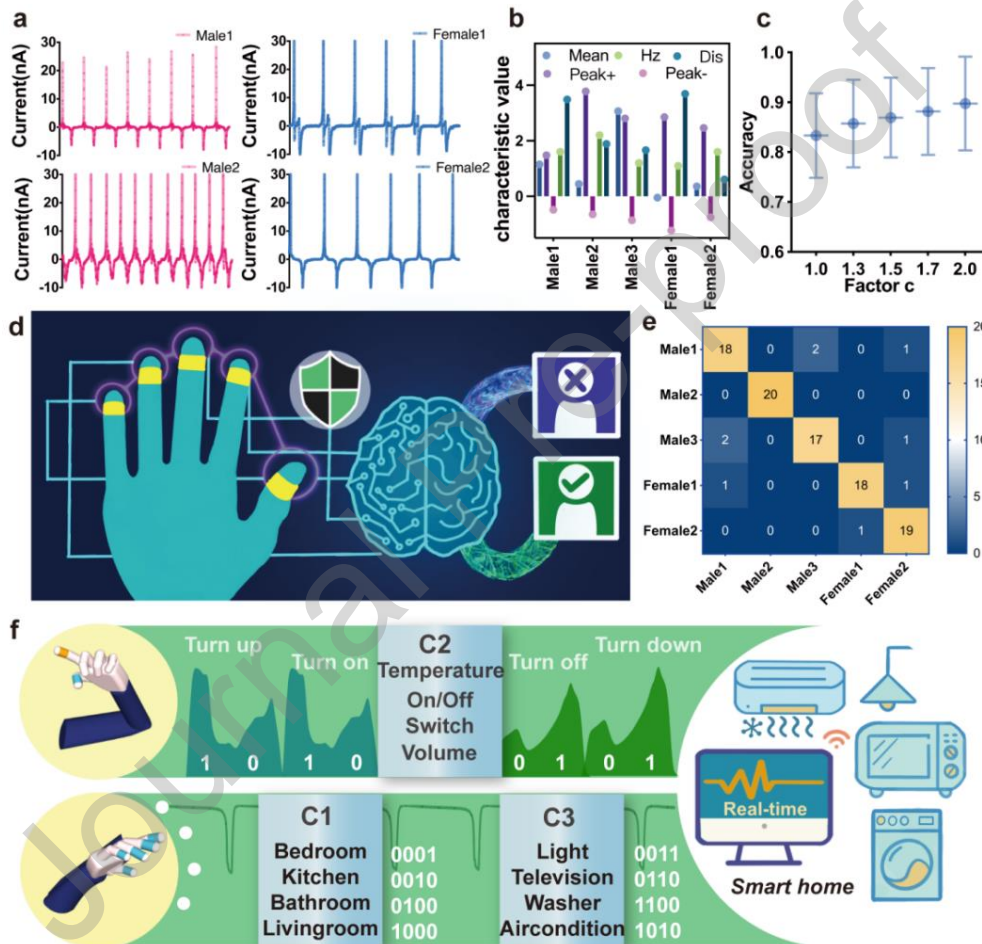


Figure 6. The extended applications of WKIS. (a) Short circuit current generated by different testers using WKIS for natural typing. (b) The obvious features that distinguish users are extracted by the algorithm. (c) Influence of the penalty coefficient C in parameter adjustment of algorithm. (d) Using WKIS to realize user identification. (e) The algorithm identifies the confusion matrix generated by the tester. (f) WKIS system is applied to smart home.

In addition to the aforementioned applications, WKIS can also be used in human-computer interaction, i.e., to help deaf people to realize the control of smart home. Figure. 6e shows the design of a home control system based on a WKIS that combines orientation and keyboard

functions. The whole system identifies the data of three modules in the order of C1-C2-C3. The control mode of C1 and C3 modules adopt finger tapping based on TENG contact-separation working mode, and the home location and the home to receive instructions are set according to the corresponding code. The C2 module enables fine step-less control via the aforementioned direction keys. Specifically, the directional data is generated via the sliding mode of the SR-TENG, whose fast response enables analog scroll-wheel type operation. The user can slide their fingers to input 10 to control the opening or raising of a parameter of C3 and input 01 to control the closing or lowering of a parameter of C3. For example, when a user with poor mobility wants to turn on the bedroom lamp, he/she only needs to input 0001 / 10 / 0011 through fingers. The whole system adopts a wireless control module, signal acquisition module, data processing module, and signal display program. With the visual interface editing through Python, the demonstration of signal control is realized (Figure. S9). The whole system is worn on one hand, which simplifies the traditional smart home system.

3. Conclusion

We have developed a WKIS based on protein electronic skin, in which silk fibroin electrode demonstrated excellent biocompatibility and skin conformal properties, enabling the device is suitable for long-term wear. Based on the difference in electronegativity between skin and PTFE, we successfully simulated the d-pad function of the keyboard by relative sliding of SR-TENG. In addition, we created a code table and successfully implanted 26 English letters into wearable devices by simple five-finger tapping. Data processing, coding, and transmission are completed through PCB and Wi-Fi modules to realize the function of WKIS communication. Then we extend the application scenario of the WKIS in user identification by support vector machine algorithm, and add the application of security identification and private information protection to the keyboard. The combination of WKIS's directional and coding functions can provide an efficient operation solution in smart home control. We believe that the programmable capabilities of WKIS will enable a wide range of application scenarios such as Internet of Things, e-skin, human machine interface and virtual reality devices.

4. Experimental Methods

Experimental design of the SF film: The SF solution with a concentration of 7wt% prepared from natural biomaterials such as silk and enhancer are mixed in a certain proportion, and no bubbles are dispersed in the Petri dish. After evaporation of water, a flat, smooth and transparent SF composite film can be formed; The reinforcing agent is generally at least one

of an organic substance (such as glycerol and cellulose) capable of improving the crystallinity of silk fibroin or a solution prepared by a hydrophilic colloid (such as polyurethane and gelatin) capable of compounding SF. Here, two enhancers, polyurethane solution, and glycerol are used to improve the performance of SF film. The specific process and ratio are as follows: glycerol is used as an enhancer and slowly dropped into silk fibroin solution at the ratio of 1:500. After mixing the solution, it is evenly coated in a clean Petri dish and evaporated naturally under the environment of 50% humidity and 26 °C for 2 days.

Experimental design of the SR-TENG: Firstly, the SF film was treated in a plasma cleaner, and then 100-200ul silver nanowire dispersion was evenly coated on its surface, and then annealed on a constant temperature heating table for 20 minutes; After annealing, lead the test end out of the silver nanowire layer with a wire, and then cover the electrode with the same SF film to package the device. The encapsulated devices can be cut according to different wearable device requirements, such as shape and size, bending angle, stretching, and extension.

Experiment measurement and characterization: XRD composition analysis: put the sample slices into the X-ray diffractometer (xenocs, xeuss 2.0) for crystal structure detection. The data parameters of the instrument are: working voltage 40 kV, working current 40 mA, target Cu K α Target, $\lambda= 0.15406$, angle measurement range is 10-80 °. Mechanical property test: place the sample on the precision micro tensile tester (microtester 5948), control the tensile tester to apply tension with an acceleration rate of 100 mm/min, and collect the tensile displacement of the material until it is pulled and broken by the strain force, to know the tensile property limit of the material. Light transmittance test: fill the sample flatly into the cuvette and place it in Shimadzu uv-3600 spectrophotometer. After removing the baseband of the cuvette itself for light absorption and reflection, test the material transmittance of light at the wavelength of 300 nm-1000 nm. Cell biocompatibility test: mouse osteoblasts MC3T3E1 were cultured on sterilized SF film samples for 3 days. The cell survival rate was tested by fluorescence staining (calcein am, sigma). The cell density of each test medium was 2×10^4 . Degradation ability test: completely immerse the sample in papain solution with a concentration of 5% and immerse it for 35 hours at room temperature until the SF film is completely degraded and disappears. TENG electrical performance test: linear motor (linmot e1100) is used to provide impact force. The triboelectric output of TENG was recorded by Keithley 6514 electrometer.

References

- [1] G. Paravati, V. Gatteschi, Human-computer interaction in smart environments, *Sensors* (Switzerland). 15 (2015) 19487–19494. <https://doi.org/10.3390/s150819487>.
- [2] M. Zhu, Z. Sun, Z. Zhang, Q. Shi, T. He, H. Liu, T. Chen, C. Lee, Haptic-feedback smart glove as a creative human-machine interface (HMI) for virtual/augmented reality applications, *Science Advances*. 6 (2020) eaaz8693. <https://doi.org/10.1126/SCIADV.AAZ8693>.
- [3] B. Dong, Z. Zhang, Q. Shi, J. Wei, Y. Ma, Z. Xiao, C. Lee, Biometrics-protected optical communication enabled by deep learning-enhanced triboelectric/photonic synergistic interface, *Science Advances*. 8 (2022) eabl9874. https://doi.org/10.1126/SCIADV.ABL9874/SUPPL_FILE/SCIADV.ABL9874_MOVIES_S1_TO_S5.ZIP.
- [4] T. Jin, Z. Sun, L. Li, Q. Zhang, M. Zhu, Z. Zhang, G. Yuan, T. Chen, Y. Tian, X. Hou, C. Lee, Triboelectric nanogenerator sensors for soft robotics aiming at digital twin applications, *Nature Communications*. 11 (2020). <https://doi.org/10.1038/s41467-020-19059-3>.
- [5] Z. Sun, M. Zhu, Z. Zhang, Z. Chen, Q. Shi, X. Shan, R.C.H. Yeow, C. Lee, Artificial Intelligence of Things (AIoT) Enabled Virtual Shop Applications Using Self-Powered Sensor Enhanced Soft Robotic Manipulator, *Advanced Science*. 8 (2021) 2100230. <https://doi.org/10.1002/advs.202100230>.
- [6] L. Xue, Z. Zhang, L. Xu, F. Gao, X. Zhao, X. Xun, B. Zhao, Z. Kang, Q. Liao, Y. Zhang, Information accessibility oriented self-powered and ripple-inspired fingertip interactors with auditory feedback, *Nano Energy*. 87 (2021) 106117. <https://doi.org/10.1016/j.nanoen.2021.106117>.
- [7] Z. Zhang, T. He, M. Zhu, Z. Sun, Q. Shi, J. Zhu, B. Dong, M.R. Yuce, C. Lee, Deep learning-enabled triboelectric smart socks for IoT-based gait analysis and VR applications, *Npj Flexible Electronics*. 4 (2020) 1–12. <https://doi.org/10.1038/s41528-020-00092-7>.
- [8] A. Haroun, X. Le, S. Gao, B. Dong, T. He, Z. Zhang, F. Wen, S. Xu, C. Lee, Progress in micro/nano sensors and nanoenergy for future AIoT-based smart home applications, *Nano Express*. 2 (2021) 022005. <https://doi.org/10.1088/2632-959x/abf3d4>.
- [9] D. Mills, F. Schroeder, J.D.' Arcy, International Conference on New Interfaces for Musical Expression GIVME: Guided Interactions in Virtual Musical Environments, (2021) 1–21.
- [10] L. Turchet, M. Barthet, An Internet of Musical Things architecture for performers-audience tactile interactions, in: *Proceedings of the Digital Music Research Network Workshop*, (2017) 1–2.

- [11] S. Kim, M. Amjadi, T.-I. Lee, Y. Jeong, D. Kwon, M.S. Kim, K. Kim, T.-S. Kim, Y.S. Oh, I. Park, Wearable, Ultrawide-Range, and Bending-Insensitive Pressure Sensor Based on Carbon Nanotube Network-Coated Porous Elastomer Sponges for Human Interface and Healthcare Devices, *ACS Applied Materials & Interfaces*. 11 (2019) 23639–23648. <https://doi.org/10.1021/acsami.9b07636>.
- [12] P. Buzing, Comparing different keyboard layouts: aspects of qwerty, dvorak and alphabetical keyboards, *Delft University of Technology Articles*. (2003) 1–11.
- [13] P.-Ola. Kristensson, *Discrete and continuous shape wrting for text entry and control*, Linköping University, 2007.
- [14] X. Su, Y. Zhang, Q. Zhao, L. Gao, Virtual keyboard: A human-computer interaction device based on laser and image processing, in: *2015 IEEE International Conference on Cyber Technology in Automation, Control, and Intelligent Systems (CYBER)*, 2015: pp. 321–325. <https://doi.org/10.1109/CYBER.2015.7287956>.
- [15] S. Pyo, J. Lee, W. Kim, E. Jo, J. Kim, Multi-Layered, Hierarchical Fabric-Based Tactile Sensors with High Sensitivity and Linearity in Ultrawide Pressure Range, *Advanced Functional Materials*. 29 (2019) 1902484. <https://doi.org/https://doi.org/10.1002/adfm.201902484>.
- [16] X. Gao, M. Zheng, X. Yan, J. Fu, Y. Hou, M. Zhu, High performance piezocomposites for flexible device application, *Nanoscale*. 12 (2020) 5175–5185. <https://doi.org/10.1039/D0NR00111B>.
- [17] W. Li, D. Torres, T. Wang, C. Wang, N. Sepúlveda, Flexible and biocompatible polypropylene ferroelectret nanogenerator (FENG): On the path toward wearable devices powered by human motion, *Nano Energy*. 30 (2016) 649–657. <https://doi.org/https://doi.org/10.1016/j.nanoen.2016.10.007>.
- [18] S.B. Jeon, S.J. Park, W.G. Kim, I.W. Tcho, I.K. Jin, J.K. Han, D. Kim, Y.K. Choi, Self-powered wearable keyboard with fabric based triboelectric nanogenerator, *Nano Energy*. 53 (2018) 596–603. <https://doi.org/10.1016/j.nanoen.2018.09.024>.
- [19] W. Yin, Y. Xie, J. Long, P. Zhao, J. Chen, J. Luo, X. Wang, S. Dong, A self-power-transmission and non-contact-reception keyboard based on a novel resonant triboelectric nanogenerator (R-TENG), *Nano Energy*. 50 (2018) 16–24. <https://doi.org/10.1016/j.nanoen.2018.05.009>.
- [20] C. Wu, W. Ding, R. Liu, J. Wang, A.C. Wang, J. Wang, S. Li, Y. Zi, Z.L. Wang, Keystroke dynamics enabled authentication and identification using triboelectric nanogenerator array, *Materials Today*. 21 (2018) 216–222. <https://doi.org/10.1016/j.mattod.2018.01.006>.

- [21] C. Hou, Z. Xu, W. Qiu, R. Wu, Y. Wang, Q. Xu, X.Y. Liu, W. Guo, A Biodegradable and Stretchable Protein-Based Sensor as Artificial Electronic Skin for Human Motion Detection, *Small*. 15 (2019) 1805084. <https://doi.org/10.1002/sml.201805084>.
- [22] J. Huang, Z. Xu, W. Qiu, F. Chen, Z. Meng, C. Hou, W. Guo, X.Y. Liu, Stretchable and Heat-Resistant Protein-Based Electronic Skin for Human Thermoregulation, *Advanced Functional Materials*. 30 (2020) 1910547. <https://doi.org/10.1002/adfm.201910547>.
- [23] Z. Xu, W. Qiu, X. Fan, Y. Shi, H. Gong, J. Huang, A. Patil, X. Li, S. Wang, H. Lin, C. Hou, J. Zhao, X. Guo, Y. Yang, H. Lin, L. Huang, X.Y. Liu, W. Guo, Stretchable, Stable, and Degradable Silk Fibroin Enabled by Mesoscopic Doping for Finger Motion Triggered Color/Transmittance Adjustment, *ACS Nano*. 15 (2021) 12429–12437. <https://doi.org/10.1021/acsnano.1c05257>.
- [24] Z. Chen, H. Zhang, Z. Lin, Y. Lin, J.H. van Esch, X.Y. Liu, Programing Performance of Silk Fibroin Materials by Controlled Nucleation, *Advanced Functional Materials*. 26 (2016) 8978–8990. <https://doi.org/10.1002/adfm.201602908>.
- [25] A.T. Nguyen, Q.L. Huang, Z. Yang, N. Lin, G. Xu, X.Y. Liu, Crystal networks in silk fibrous materials: From hierarchical structure to ultra performance, *Small*. 11 (2015) 1039–1054. <https://doi.org/10.1002/sml.201402985>.
- [26] H. Tu, R. Yu, Z. Lin, L. Zhang, N. Lin, W.D. Yu, X.Y. Liu, Programing Performance of Wool Keratin and Silk Fibroin Composite Materials by Mesoscopic Molecular Network Reconstruction, *Advanced Functional Materials*. 26 (2016) 9032–9043. <https://doi.org/10.1002/adfm.201603403>.
- [27] H. Gong, Z. Xu, Y. Yang, Q. Xu, X. Li, X. Cheng, Y. Huang, F. Zhang, J. Zhao, S. Li, X. Liu, Q. Huang, W. Guo, Transparent, stretchable and degradable protein electronic skin for biomechanical energy scavenging and wireless sensing, *Biosensors and Bioelectronics*. 169 (2020) 112567. <https://doi.org/10.1016/j.bios.2020.112567>.
- [28] J.J. Shao, T. Jiang, Z.L. Wang, Theoretical foundations of triboelectric nanogenerators (TENGs), *Science China Technological Sciences*. 63 (2020) 1087–1109. <https://doi.org/10.1007/s11431-020-1604-9>.
- [29] S. Niu, Z.L. Wang, Theoretical systems of triboelectric nanogenerators, *Nano Energy*. 14 (2014) 161–192. <https://doi.org/10.1016/j.nanoen.2014.11.034>.
- [30] H. Zou, Y. Zhang, L. Guo, P. Wang, X. He, G. Dai, H. Zheng, C. Chen, A.C. Wang, C. Xu, Z.L. Wang, Quantifying the triboelectric series, *Nature Communications*. 10 (2019) 1–9. <https://doi.org/10.1038/s41467-019-09461-x>.

- [31] J. Shao, T. Jiang, W. Tang, X. Chen, L. Xu, Z.L. Wang, Structural figure-of-merits of triboelectric nanogenerators at powering loads, *Nano Energy*. 51 (2018) 688–697. <https://doi.org/10.1016/j.nanoen.2018.07.032>.
- [32] P.S. Teh, A.B.J. Teoh, S. Yue, A survey of keystroke dynamics biometrics, *The Scientific World Journal*. 2013 (2013) 408208. <https://doi.org/10.1155/2013/408280>.
- [33] M.L. Ali, J. v. Monaco, C.C. Tappert, M. Qiu, Keystroke Biometric Systems for User Authentication, *Journal of Signal Processing Systems*. 86 (2017) 175–190. <https://doi.org/10.1007/s11265-016-1114-9>.
- [34] F. Monrose, A.D. Rubin, Keystroke dynamics as a biometric for authentication, 2000.
- [35] Q. Liu, C. Chen, Y. Zhang, Z. Hu, Feature selection for support vector machines with RBF kernel, *Artificial Intelligence Review*. 36 (2011) 99–115. <https://doi.org/10.1007/s10462-011-9205-2>.
- [36] S. Han, C. Qubo, H. Meng, Parameter selection in SVM with RBF kernel function, in: *World Automation Congress 2012*. (2012) 1–4

Acknowledgements

This work was supported by the National Nature Science Foundation of China (22175146, 52001265), Key research and development project of Jiangxi province (20212BBG73007), the Guangdong Natural Science Foundation (2021A1515010680), the Fundamental Research Funds for the Central Universities of China (20720210027, 20720222004), the “111” Project (B16029), Visiting Scholar Fund of Key Laboratory of Optoelectronic Technology & Systems (Chongqing University).

Author Contributions

J.L. and W.G. designed SR-TENG and WKIS, conducted the experiments, analyzed data, and wrote the manuscript. S.L. and J.Z. prepared the materials and conducted the SR-TENG wearable tests. J.L., J.C. and F.D. trained the machine learning model, and developed the WKIS system. Y.S. conducted the biocompatibility experiments. W.L., L.G. conducted the WKIS data acquisition tests. W.G., Y.L. and X.C. developed the experimental programs, directed the study and edited the manuscript.

Data Availability

All data needed to evaluate the conclusions in the paper are present in the paper and/or the Supplementary Materials. Additional data related to this paper may be requested from the authors.

Competing Interests

Authors declare that they have no competing interests.

Graphical Abstract



We report a new generation wearable keyboardless input system (WKIS), which consists of only five triboelectric nanogenerator (TENG) rings worn on the fingers. With the help of our original vowel mode input method, 26 English letters can be input without keyboard by simple five-finger tapping. Data coding and transmission process are completed through a printed circuit board (PCB) and Wi-Fi module to realize keyboard communication. Feature engineering and machine learning are employed to identify WKIS registered users with an accuracy of 92%.

Credit Author Statement

J.L. and W.G. designed SR-TENG and WKIS, conducted the experiments, analyzed data, and wrote the manuscript. S.L. and J.Z. prepared the materials and conducted the SR-TENG wearable tests. J.L., J.C. and F.D. aitrained the machine learning model, and developed the WKIS system. Y.S. conducted the biocompatibility experiments. W.L., L.G. conducted the WKIS data acquisition tests. W.G., Y.L. and X.C. developed the experimental programs, directed the study and edited the manuscript.

Declaration of interests

The authors declare that they have no known competing financial interests or personal relationships that could have appeared to influence the work reported in this paper.

The authors declare the following financial interests/personal relationships which may be considered as potential competing interests:

Highlights

- Biocompatible, water/air permeable and ultra-thin triboelectric nanogenerator (TENG) based on silk fibroin film (SF) is fabricated.
- Unique vowel mode input method is developed to integrate 26 English letters and necessary instructions into wearable keyboard with five-finger tapping.
- Human-computer interaction and private information protection are realized by a printed circuit board, Wi-Fi module and machine learning.